3-D Ultrasound Imaging Using Forward Viewing CMUT Ring Arrays for Intravascular and Intracardiac Applications

David T. Yeh*, Ömer Oralkan*, Ira O. Wygant*, Matthew O'Donnell†, and Butrus T. Khuri-Yakub*
*Edward L. Ginzton Laboratory
Stanford University, Stanford, CA 94305–4088
Email: dtyeh@stanford.edu
†Biomedical Engineering Department
University of Michigan, Ann Arbor, MI 48019–2099

***Abstract*— Forward-viewing ring arrays can enable new applications in intravascular and intracardiac ultrasound. We have demonstrated full synthetic phased array volumetric ultrasound imaging using a forward-viewing CMUT ring array with 64 elements, in both the conventional (8 MHz) and collapse (19 MHz) regimes of operation. Measured SNR of an echo from a plane reflector at 5 mm is 29 dB for 8 MHz and 35 dB for 19 MHz. The 6-dB axial and lateral resolutions for the B-scan of the wire target is 189 μm and 0.112 radians for 8 MHz, and 78 μm and 0.051 radians for 19 MHz. Rendered 3-D images of a Palmaz-Schatz stent are also shown, demonstrating that the imaging quality is sufficient for clinical applications.**

I. Introduction

Forward-viewing intravascular ultrasound enables new procedures in medicine such as diagnosing severely occluded blood vessels or guiding the placement of stents. A ring-shaped forward-viewing transducer provides clearance for the guidewire in catheter-based applications. Also, the forward-viewing ring array is capable of volumetric imaging, which is highly desirable because it reduces operator dependence in clinical ultrasound.

Previous efforts have found it challenging to design and fabricate ring arrays using piezoelectric transducers with sufficient performance in the forward-looking mode [1]. Consequently, there have been several efforts to make ring arrays using Capacitive Micromachined Ultrasonic Transducers (CMUTs) with the goal of volumetric intravascular ultrasound [2], [3]. This paper presents the characterization of a CMUT ring array and its imaging capabilities.

II. CMUT Ring Arrays

CMUTs offer several advantages over piezoelectric transducers for use in medical imaging [4]. The microlithography process used to make CMUTs churns out batches of transducers with the fine dimensions required for high-frequency ring arrays. The wide bandwidth of CMUTs in immersion improves the resolution of ultrasound images.

Operating the CMUT in collapse affords particularly good characteristics for imaging, including higher echo signal levels and higher frequency [5]. In addition, the CMUT can be switched between its two operating modes during the imaging procedure. The operator can choose conventional mode operation for lower frequency and better penetration for navigation, or collapse mode for higher frequency and resolution for diagnosis.

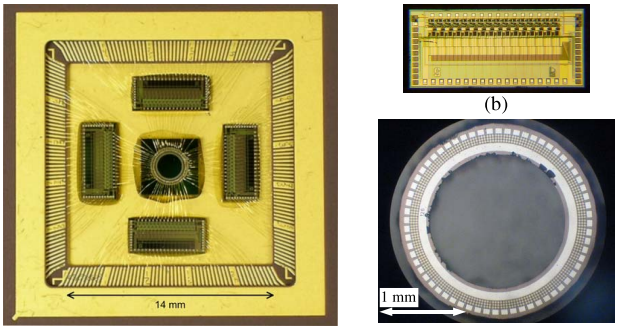

Fig. 1. (a) Ring array wire bonded to electronics; (b) 16-channel transmit/receive circuit; (c) 64-element CMUT ring array.

The parameters for the CMUT ring array presented are as follows: ring diameter, 2 mm; number of elements, 64; element pitch, 102 μm; element size, 100×100 μm; cells per element, 9; cell membrane radius, 13 μm; electrode radius, 9 μm; membrane thickness, 0.4 μm; gap distance, 0.15 μm; collapse voltage, 50 V. The very small element area required for this application makes ultrasound imaging difficult, yet the CMUT provides sufficient performance to produce clear images.

III. Experimental Setup

Four integrated circuits, with 16 independent pulsers and amplifiers each, were wire bonded to the elements of the CMUT in a 209 pin grid array (PGA) electronics package, as shown in Fig. 1. Although this arrangement is capable of full phased array operation, full synthetic phased array imaging was performed to simplify the data collection and to acquire the most general data set for offline reconstruction with various beamforming schemes. The CMUT was biased at 30 V for

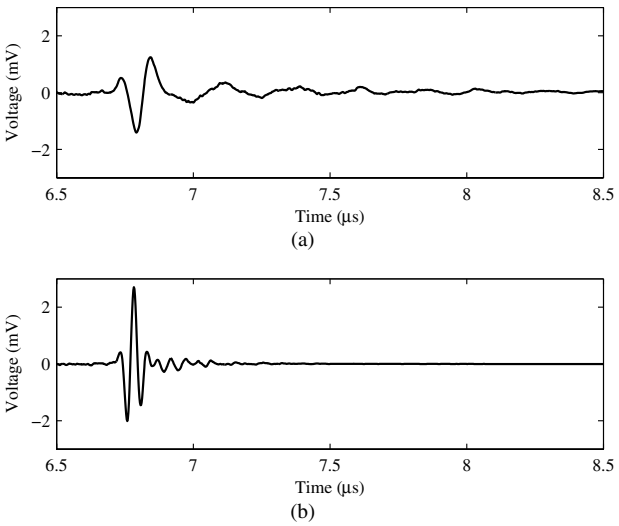

Fig. 2. Pulse-echo response: (a) Conventional; (b) Collapse mode;

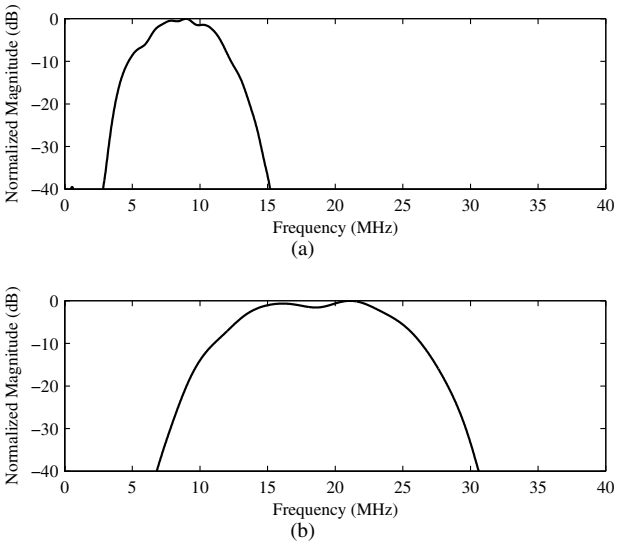

Fig. 3. FFT of filtered pulse-echo response: (a) Conventional; (b) Collapse mode.

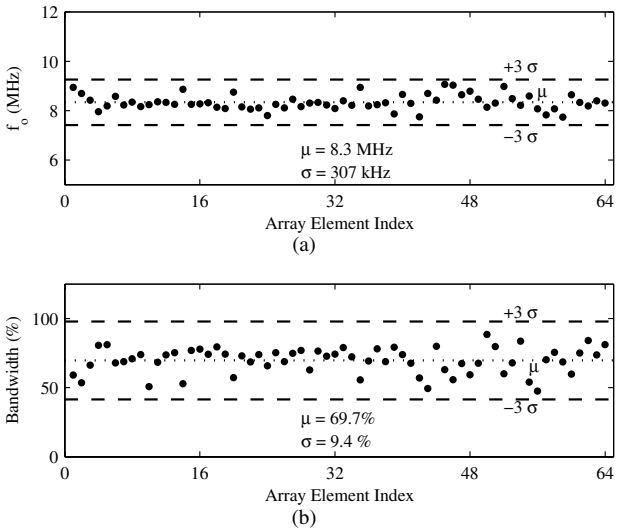

Fig. 4. Uniformity across ring array, conventional mode: (a) Center frequency; (b) Fractional bandwidth.

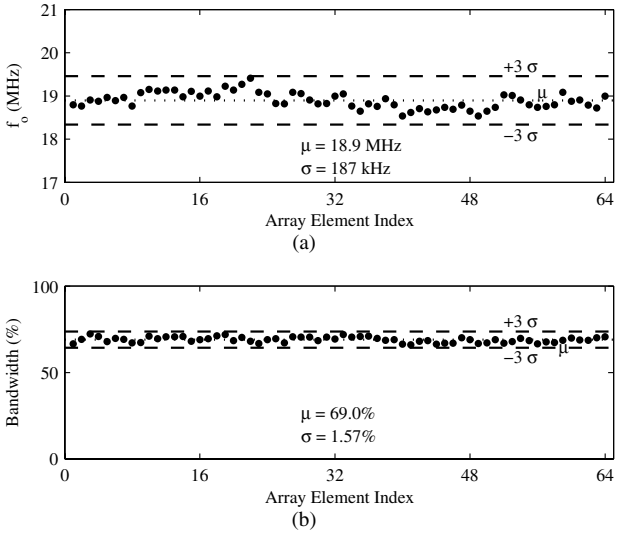

Fig. 5. Uniformity across ring array, collapse mode: (a) Center frequency; (b) Fractional bandwidth.

conventional operation and 100 V for collapse mode. Elements were excited one at a time with a 25-V pulse, and A-scans were acquired from the entire array for each transmit element. Each A-scan was collected at a sampling rate of 500 MS/s for both conventional and collapse mode operation, and using 16 averages.

IV. Results

A. A-Scan Results

Pulse-echo data of a plane reflector (the oil-air interface) at 5 mm was taken from a single element. For the conventional case, the pulse width was 60 ns; for collapse mode, the pulse width was 27 ns. The echo, shown in Fig. 2, demonstrates the wide bandwidth of the CMUT. Fig. 3 shows the FFT of the pulse-echo signal after it has been filtered using a Gaussian bandpass filter with a 6-dB band from 5.5 to 13 MHz for conventional, and 10 to 27.5 MHz for collapse. In conventional mode, the device operates at 8.3 MHz with a 6-dB fractional bandwidth of 70%, and in collapse, 19 MHz with a fractional bandwidth of 69%. The SNR of a plane reflector at 5 mm is 29 dB for conventional and 35 dB for collapse.

B. Imaging Results

A conical volume was reconstructed offline using the full 64×64 set of A-scans from an imaging target with weightings for full-aperture resolution [6] and cosine apodization. All images are shown with 40 dB of dynamic range. The imaging phantom is shown in Fig. 6, and consists of three steel wires, each 0.3 mm in diameter. Fig. 7 shows the Y-Z and X-Z planes of the conical volume (depicted in Fig. 6). Because of the higher frequency and reduced acoustic crosstalk, collapse mode produces images with a narrower main lobe and fewer

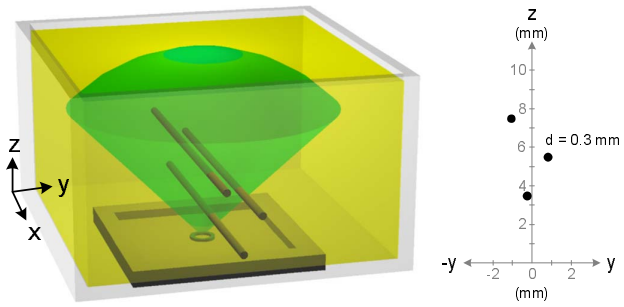

Fig. 6. Phantom of three wires.

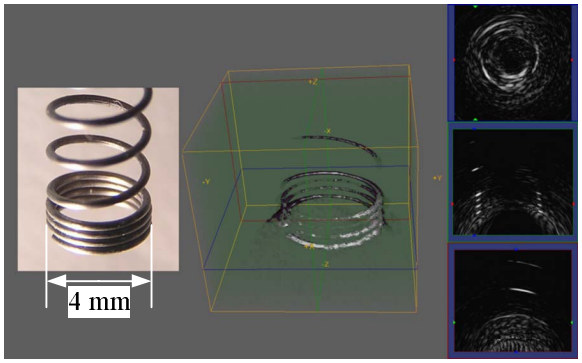

Fig. 9. Photograph of spring, 3-D rendered ultrasound of spring, cross sections with 40 dB dynamic range.

artifacts than conventional mode imaging. The image SNR in conventional is 50 dB compared to 22 dB for the SNR of the wire A-scan. In collapse mode, the image SNR is 48 dB and the A-scan SNR, 24 dB.

The experimental axial and lateral line spread functions (LSF) of the array are shown in Fig. 8 alongside the simulated results. The 6-dB axial and lateral resolutions for for the B-scan of the wire target is 189 μm and 0.112 radians for 8 MHz, and 78 μm and 0.051 radians for 19 MHz.

Finally, volume images of several targets were generated and are shown in Figs. 9,10,11 to exhibit the quality of images produced by this ring array.

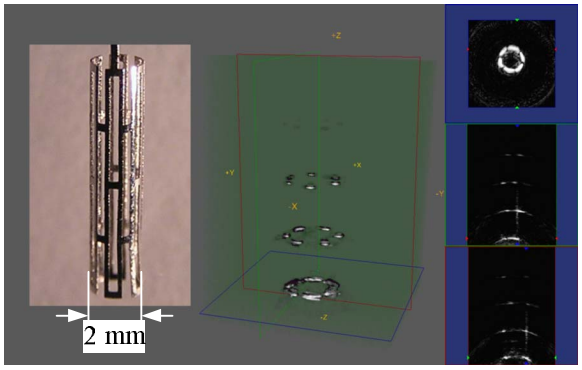

Fig. 10. Photograph of Palmaz-Schatz stent, undeployed, 3-D rendered ultrasound of stent, cross sections with 40 dB dynamic range.

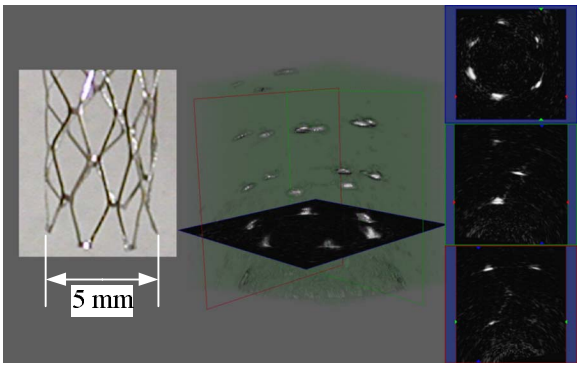

Fig. 11. Photograph of Palmaz-Schatz stent, deployed, 3-D rendered ultrasound of stent, cross sections with 40 dB dynamic range.

V. Conclusion

We have demonstrated volumetric ultrasound imaging with a forward-viewing CMUT ring array. Future work involves developing a fully integrated system with flip-chip bonded electronics for incorporation into a catheter probe. These results show that CMUT ring arrays with custom front-end integrated circuits can produce images with ample quality for clinical use.

Acknowledgment

This work was supported by the National Institutes of Health. Thanks to Bill Broach and the Portable Power group at National Semiconductor Corporation for supporting us with assistance in circuit design and for providing the custom integrated circuits. Thanks to Volcano Therapeutics for providing the stents. David Yeh is supported by a National Defense Science and Engineering Graduate Fellowship.

References

[1] Y. Wang, D. Stephens, and M. O'Donnell, "Initial results from a forward-viewing ring-annular ultrasound array for intravascular imaging," in *Proc. IEEE Ultrason. Symp.*, vol. 1, Oct. 2003, pp. 212–215.

[2] U. Demirci, A. S. Ergun, Ö. Oralkan, M. Karaman, and B. T. Khuri-Yakub, "Forward-viewing CMUT arrays for medical imaging." *IEEE Trans. Ultrason., Ferroelect., Freq. Contr.*, vol. 51, no. 7, pp. 887–895, July 2004.

[3] F. L. Degertekin, R. O. Guldiken, and M. Karaman, "Micromachined capacitive transducer arrays for intravascular ultrasound," in *Proc. SPIE MOEMS Display and Imaging Systems III*, vol. 5721, no. 1, San Jose, CA, 2005, pp. 104–114.

[4] Ö. Oralkan, A. S. Ergun, J. A. Johnson, U. Demirci, M. Karaman, K. Kaviani, T. H. Lee, and B. T. Khuri-Yakub, "Capacitive micromachined ultrasonic transducers: Next-generation arrays for acoustic imaging?" *IEEE Trans. Ultrason., Ferroelect., Freq. Contr.*, vol. 49, no. 11, pp. 1596–1610, Nov. 2002.

[5] B. Bayram, E. Hæggström, G. G. Yaralioglu, and B. T. Khuri-Yakub, "A new regime for operating capacitive micromachined ultrasonic transducers," *IEEE Trans. Ultrason., Ferroelect., Freq. Contr.*, vol. 50, no. 9, pp. 1184–1190, Sept. 2003.

[6] S. J. Norton, "Annular array imaging with full-aperture resolution," *J. Acoust. Soc. Am.*, vol. 92, no. 6, pp. 3202–3206, Dec. 1992.

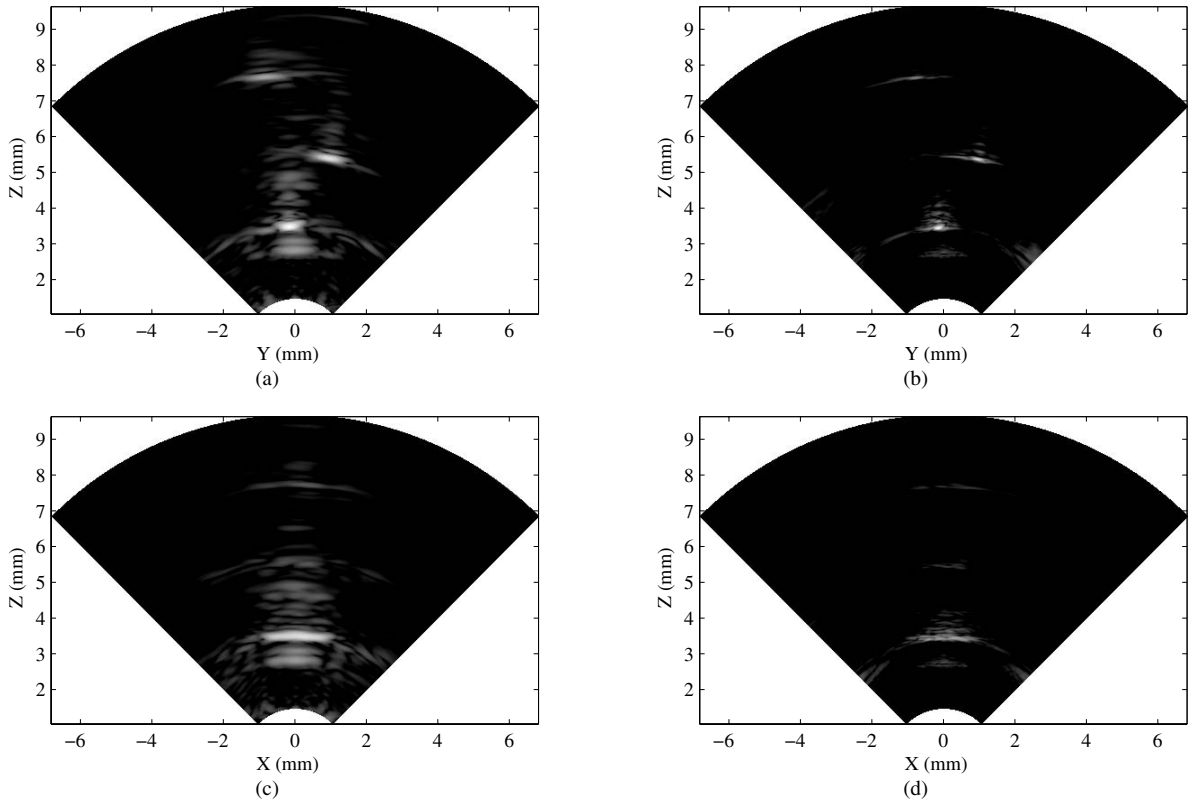

Fig. 7. Slices of 3-D volume, 40 dB range: (a) Y-Z plane, conventional; (b) Y-Z plane, collapse mode; (c) X-Z plane, conventional; (d) X-Z plane, collapse mode.

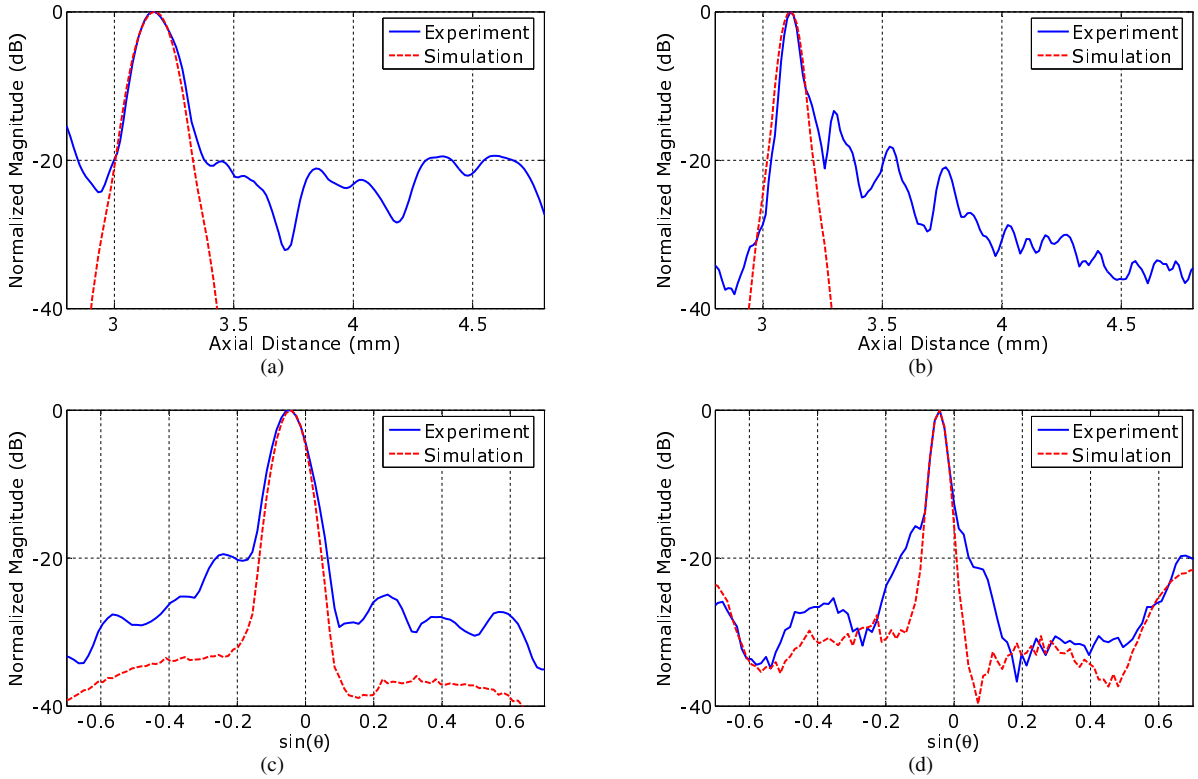

Fig. 8. Experimental versus simulated line spread functions: (a) Axial LSF, conventional; (b) Axial LSF, collapse mode; (c) Lateral LSF, conventional; (d) Lateral LSF, collapse mode.